

Magnetic dynamo action in astrophysical turbulence

Leonid Malyshkin¹ and Stanislav Boldyrev²

¹*Department of Astronomy & Astrophysics, University of Chicago, 5640 S. Ellis Ave., Chicago, IL 60637; leonmal@uchicago.edu*

²*Department of Physics, University of Wisconsin-Madison, 1150 University Ave., Madison, WI 53706; boldyrev@wisc.edu*

ABSTRACT

We investigate the structure of magnetic field amplified by turbulent velocity fluctuations, in the framework of the kinematic Kazantsev-Kraichnan model. We consider Kolmogorov distribution of velocity fluctuations, and assume that both Reynolds number and magnetic Reynolds number are very large. We present the full numerical solution of the model for the spectra and the growth rates of magnetic fluctuations. We consider astrophysically relevant limits of large and small magnetic Prandtl numbers, and address both helical and nonhelical cases.

Subject headings: magnetic fields — magnetohydrodynamics: MHD — turbulence

1. Introduction

Magnetic fields are found everywhere in the universe, in planets and stars, in galaxies and galaxy clusters. Magnetic fields in astrophysical systems are usually generated in a broad interval of scales, ranging from small resistive scales to large scales exceeding the correlation length of plasma motions. One of the most important, challenging and still open questions in astrophysics is how cosmic magnetic fields have been generated and what is their structure. The prevailing theory for the origin of magnetic fields is dynamo action, which is stretching of magnetic field lines by random motion of highly conducting plasmas or fluids in which these lines are frozen (e.g., Vainshtein & Zeldovich 1972; Parker 1979; Lynden-Bell 1994; Zweibel & Heiles 1997; Brandenburg & Subramanian 2005; Kulsrud 2005; Schekochihin & Cowley 2006; Kulsrud & Zweibel 2008). Small-scale magnetic fields, that is fields at the scales smaller than the velocity field scales, are generally expected under this mechanism, while large-scale magnetic fields, correlated at scales larger than the correlation scale of a velocity field, can be generated if some additional conditions are met, such as

the condition that the velocity field $\mathbf{v}(\mathbf{x}, \mathbf{t})$ is not mirror symmetric, say, possesses nonzero kinetic helicity $H = \int \mathbf{v} \cdot (\nabla \times \mathbf{v}) d^3x \neq 0$ (Steenbeck, Krause & Radler 1966; Moffatt 1978).

Assume that the velocity fluctuations have the typical correlation scale l_0 , and the typical rms value v_0 , and the plasma has kinematic viscosity ν and magnetic diffusivity η (the latter is proportional to electrical resistivity). The range of scales available for velocity and magnetic fluctuations can be characterized by the Reynolds number $\text{Re} \sim l_0 v_0 / \nu$ and the magnetic Reynolds number $\text{Rm} \sim l_0 v_0 / \eta$, respectively. In astrophysical applications both numbers are very large (for example, in a protogalaxy, where dynamo action is believed to operate, Re and Rm reach values $\sim 10^5$ and $\sim 10^{26}$, respectively). Their ratio, the magnetic Prandtl number $\text{Pm} = \text{Rm} / \text{Re}$ can be either large or small. For example, in galaxies and galaxy clusters $\text{Pm} \gg 1$, while in planets and stellar interiors $\text{Pm} \ll 1$. Because of the vast range of scales available for magnetic and velocity fluctuations, and generally strongly disparate magnetic and velocity dissipation scales, present-day direct numerical simulations cannot directly address astrophysical magnetohydrodynamic (MHD) regimes. Indeed, maximal Reynolds and magnetic Reynolds numbers accessible with numerical simulations are hopelessly small, of the order of $10^3 - 10^4$, in which case the typical magnetic Prandtl numbers are not significantly different from $\text{Pm} \sim 1$. A physical picture of magnetic dynamo action and an effective analytic framework for investigating astrophysical dynamo action are therefore in demand.

The first step in understanding dynamo action is to understand the initial, kinematic stage of magnetic field amplification. In this regime, the magnetic field is weak and does not affect the velocity fluctuations. Magnetic field evolution is therefore fully described by the induction equation in which the velocity field is prescribed independently of the magnetic field. An effective framework in this case is provided by the so-called Kazantsev-Kraichnan model, where the velocity field is assumed to be a random Gaussian short-time-correlated field. This formal simplification allows for analytic solutions of the model while capturing the essential physics of the phenomenon. We should note however that even with this simplification the model is nontrivial and its general solution is not known. Only certain special cases have been solved so far, which reveal a good agreement with numerical simulations in the parameter range accessible to numerics (e.g., Maron & Cowley 2001; Haugen, Brandenburg & Dobler 2004; Boldyrev & Cattaneo 2004).

The Kazantsev-Kraichnan dynamo model allows one to answer the fundamental questions concerning the possibility of turbulent dynamo action for given Reynolds and magnetic Reynolds numbers, the spectrum of growing magnetic fluctuations, the conditions for large-scale magnetic field amplification, etc. In many instances, the results obtained in high-resolution numerical simulations were predicted by the model well before such simulations

become available. We therefore believe that the model can provide a valuable insight into astrophysical dynamo regimes that can hardly be accessed through direct numerical simulations in foreseeable future.

Our preliminary results aimed at the full numerical characterization of the kinematic dynamo action in the Kazantsev-Kraichnan framework were presented in Malyshkin & Boldyrev (2007). In particular, we investigated the growth rates of magnetic fluctuations in the velocity field with the Kolmogorov energy spectrum. In the present paper, we explore the spatial structure of the growing magnetic eigenmodes. We assume the Kolmogorov spectrum of velocity fluctuations and address extremely large Reynolds numbers, up to $\text{Re} \sim 10^9$. This allows us to study astrophysically relevant limits of very large and very small magnetic Prandtl numbers. For completeness, we perform our analysis for the cases of both large and small kinetic helicity. In the helical case we also discuss the relevance of the conventional α -model for the description of large-scale dynamo action, in the case when small-scale magnetic fluctuations are amplified as well.

In the next section, we describe the Kazantsev-Kraichnan model of kinematic dynamo action. In Section 3, we present our results, and in Section 4 we give our conclusions.

2. Kazantsev-Kraichnan model

Kinematic dynamo action is described by the induction equation for the magnetic field:

$$\partial_t \mathbf{B} = \nabla \times (\mathbf{v} \times \mathbf{B}) + \eta \nabla^2 \mathbf{B}, \quad (1)$$

where $\mathbf{v}(\mathbf{x}, t)$ is the velocity field, $\mathbf{B}(\mathbf{x}, t)$ is the magnetic field, and η is the magnetic diffusivity. In this equation the velocity field is prescribed independently of the magnetic field. Following Kazantsev (1968) and Kraichnan (1968), we assume that the velocity field is statistically homogeneous and isotropic and has a Gaussian distribution with zero mean, $\langle \mathbf{v} \rangle = 0$, and the following covariance tensor

$$\langle v^i(\mathbf{x}, t) v^j(\mathbf{x}', t') \rangle = \kappa^{ij}(\mathbf{x} - \mathbf{x}') \delta(t - t'), \quad (2)$$

where κ^{ij} is an isotropic tensor of turbulent diffusivity,

$$\kappa^{ij}(\mathbf{x}) = \kappa_N \left(\delta^{ij} - \frac{x^i x^j}{x^2} \right) + \kappa_L \frac{x^i x^j}{x^2} + g \epsilon^{ijk} x^k. \quad (3)$$

Here, functions $\kappa_L(x)$ and $g(x)$ describe kinetic energy and helicity, $x = |\mathbf{x}|$, brackets $\langle \rangle$ denote ensemble average, ϵ^{ijk} is the unit antisymmetric pseudotensor and summation over

repeated indices is assumed. The first two terms on the right-hand side of Equation (3) represent the mirror-symmetric, nonhelical part, while the last term describes the helical part of the velocity fluctuations. For an incompressible velocity field (the only case we consider here), we have $\kappa_N(x) = \kappa_L(x) + x\kappa'_L(x)/2$, where the prime denotes derivative with respect to $x = |\mathbf{x}|$. Therefore, to describe the velocity field, we specify only two independent functions, $\kappa_L(x)$ and $g(x)$. The Fourier transformation of Equation (3) is

$$\kappa^{ij}(\mathbf{k}) = F(k) \left(\delta^{ij} - \frac{k^i k^j}{k^2} \right) + iG(k) \epsilon^{ijl} k^l. \quad (4)$$

Functions $F(k)$ and $G(k)$ can be obtained from functions $\kappa_L(x)$ and $g(x)$, and vice versa, by using the three-dimensional Fourier transforms (Monin & Yaglom 1971).

The correlator of homogeneous and isotropic magnetic field can similarly be expressed as

$$\langle B^i(\mathbf{x}, t) B^j(0, t) \rangle = M_N \left(\delta^{ij} - \frac{x^i x^j}{x^2} \right) + M_L \frac{x^i x^j}{x^2} + K \epsilon^{ijk} x^k, \quad (5)$$

where the field solenoidality constraint $\text{div } \mathbf{B} = 0$ implies $M_N(x, t) = M_L(x, t) + (x/2)M'_L(x, t)$. To fully describe the magnetic field correlator, we need to find only two functions, $M_L(x, t)$ and $K(x, t)$, corresponding to magnetic energy and magnetic helicity. The Fourier transformed version of Equation (5) is

$$\langle B^i(\mathbf{k}, t) B^{*j}(\mathbf{k}, t) \rangle = F_B(k, t) \left(\delta^{ij} - \frac{k^i k^j}{k^2} \right) - i \frac{H_B(k, t)}{2k^2} \epsilon^{ijl} k^l, \quad (6)$$

where $F_B(k, t)$ is the magnetic energy spectral function, $\langle |\mathbf{B}(\mathbf{k}, t)|^2 \rangle = 2F_B(k, t)$, and $H_B(k, t)$ is the spectral function of the electric current helicity, $\langle B^{i*}(\mathbf{k}, t) i \epsilon^{ijl} k^j B^l(\mathbf{k}, t) \rangle = H_B(k, t)$. The problem is then to find the correlation function (Equation (5)) of the magnetic field, or, alternatively, its Fourier version (Equation (6)).

Suppose that the velocity field (Equations (2) and (3)) is given, i.e., kinetic energy $\kappa_L(x)$ and kinetic helicity $g(x)$ are given. In this case, to find the properties of the growing magnetic field driven by helical dynamo action, one needs to solve two coupled partial differential equations for functions $M_L(x, t)$ and $K(x, t)$ related to magnetic energy and magnetic helicity. Such equations were first derived by Vainshtein & Kichatinov (1986). Due to their complexity, there have been few theoretical results obtained for the helical dynamo (e.g., Kulsrud & Anderson 1992; Kim & Hughes 1997; Blackman & Field 2002). For direct numerical simulations see Brandenburg & Subramanian (2005) and references therein. Recently, it has been established in Boldyrev, Cattaneo & Rosner (2005) that Vainshtein & Kichatinov (1986) equations also possess a self-adjoint structure, which is similar to a two-component quantum mechanical “spinor” form with imaginary time. These two

coupled self-adjoint differential equations are linear and homogeneous, and they describe the growth of the magnetic field in the Kazantsev-Kraichnan model with nonzero kinetic helicity. We solve them numerically by the fourth-order Runge-Kutta integration method and by matching the numerical solution to the analytical asymptotic solutions at $x \rightarrow 0$ and $x \rightarrow \infty$, for details see Malyshkin & Boldyrev (2007).

We are interested in fast exponentially growing eigenmodes of the magnetic field amplified by helical kinematic dynamo. Therefore, both magnetic correlator functions $M_L(x, t)$ and $K(x, t)$ are assumed to be proportional to $\exp(\lambda t)$, where λ is the growth rates of the field eigenmodes. It is important that Boldyrev, Cattaneo & Rosner (2005) helical dynamo equations, which we solve, are self-adjoint because this guarantees that all growth rates λ are real. It turns out that in analogy with quantum mechanics, there are two types of magnetic field eigenmodes: bound (spatially localized) and unbound (spatially nonlocalized). First, for growth rates $\lambda > \lambda_0 \equiv g^2(0)/[\kappa_L(0) + 2\eta]$ the eigenfunctions are bound and correspond to “particles” trapped by the potential provided by velocity fluctuations. The bound eigenmodes have discrete growth rates, i.e., $\lambda = \lambda_n > \lambda_0$ where $n = 1, 2, 3, \dots$. The bound eigenfunctions decline exponentially to zero as $x \rightarrow \infty$. Second, for $\lambda \leq \lambda_0$ the eigenfunctions are unbound and correspond to “traveling particles”. The unbound eigenmodes have continuous eigenvalues of their growth rates, $0 < \lambda \leq \lambda_0$. The unbound eigenfunctions asymptotically become a mixture of cosine and sine standing waves as $x \rightarrow \infty$. Eigenvalue λ_0 corresponds to the fastest growing unbound eigenmode. The structure and other properties of the magnetic field amplified by dynamo action are fully determined by all growing eigenmodes of the magnetic field. In particular, the magnetic energy spectral function $F_B(k, t)$ is the sum over all energy spectral eigenfunctions,

$$\langle |\mathbf{B}(\mathbf{k}, t)|^2 \rangle / 2 = F_B(k, t) = \sum_{n=1}^{n_{\max}} c_n F_{B,n}(k, t) + \int_0^{\lambda_0} c(\lambda) F_{B,\lambda}(k, t) d\lambda. \quad (7)$$

In this equation $F_{B,n}(k, t)$ and $F_{B,\lambda}(k, t)$ are the energy spectral eigenfunctions for the bound and unbound eigenmodes, respectively; coefficients c_n and $c(\lambda)$ depend on the seed magnetic field at the initial moment when dynamo started to operate.¹ Similarly to Equation (7), the electric current helicity spectral function $H_B(k, t)$ is the sum over all helicity spectral eigenfunctions with the same coefficients as in Equation (7). To find the correlation function of the magnetic field, it is sufficient to find all growth rates and the corresponding spectral eigenfunctions.

¹ Note that while the energy spectrum $F_B(k, t) = \langle |\mathbf{B}(\mathbf{k}, t)|^2 \rangle / 2$ stays always positive, the individual energy spectral eigenfunctions can be negative. The sharp declines in individual eigenfunctions $F_B(k)$ and $H_B(k)$ plotted in Figures 2 and 3 are due to the logarithmic representation of the eigenfunctions in these figures, which has difficulty to suit with values $F_B(k) = 0$ and $H_B(k) = 0$.

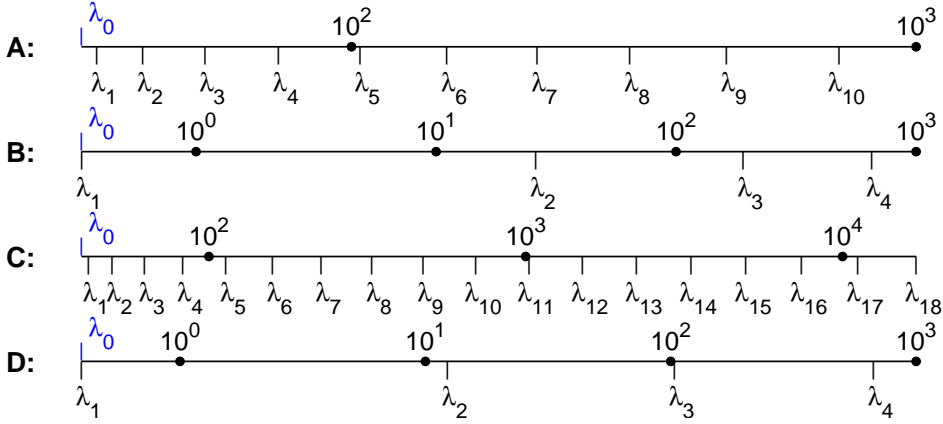


Fig. 1.— Growth rates λ_n of the bound magnetic eigenmodes, and λ_0 of the fastest growing unbound eigenmode. Plots (A) and (B) are for $h = 1$ and 0.1 , respectively, while $k_{\max} = 3000$ (Reynolds number $\text{Re} \gg 1$ and Prandtl number $\text{Pm} \gg 1$). Plots (C) and (D) are for $h = 1$ and 0.1 , respectively, while $k_{\max} = 3 \times 10^7$ ($\text{Re} \gg 1$ and $\text{Pm} \ll 1$). All plots are on the logarithmic scale.

3. Results

To study a case relevant to astrophysical systems, we consider velocity correlation tensor (Equation (4)) with the Kolmogorov power velocity spectrum and large Reynolds number, $\text{Re} \gg 1$. In the Kolmogorov turbulence, the turbulent diffusivity, given by Equation (3), scales as $v_l l \sim l^{4/3}$, where $l = |\mathbf{x} - \mathbf{x}'|$ (see, e.g., Frisch 1995). As a result, the Kolmogorov scaling implies $\kappa_L(x) \approx \kappa(0)(x/l_0)^{4/3} \approx v_0 l_0 (x/l_0)^{4/3}$. Without loss of generality we take $l_0 \sim 1$, $v_0 \sim 1$, and therefore

$$\begin{aligned} F(k) &= k^{-13/3}, \\ G(k) &= -hk^{-1}F(k), \end{aligned} \quad 2 \leq k \leq k_{\max}. \quad (8)$$

Here, the lower cutoff wavenumber is $k_{\min} = 2$, the upper cutoff wavenumber $k_{\max} \approx 2[\kappa_L(0)/\nu]^{3/4} \approx 4\nu^{-3/4}$ is determined by the plasma kinematic viscosity ν , and the helicity parameter h must satisfy the realizability condition $-1 \leq h \leq 1$; the velocity field is maximally helical when $|h| = 1$.²

We choose magnetic diffusivity to be $\eta = 10^{-6}$, corresponding to magnetic Reynolds number $\text{Rm} \sim 10^6$. By changing the value of the turbulence cutoff wavenumber k_{\max} in

² Given $\kappa_L(x)$, function $g(x)$ cannot be chosen arbitrarily, its Fourier image must satisfy the realizability condition $|G(k)| \leq F(k)/k$ (Moffatt 1978). This results in the condition $-1 \leq h \leq 1$. Analogously, given $M_L(x, t)$, function $K(x, t)$ is restricted by condition $|H_B(k, t)| \leq 2kF_B(k, t)$.

Equation (8), we vary the Reynolds number $\text{Re} \approx 1/\nu \approx (k_{\text{max}}/4)^{4/3}$ and the magnetic Prandtl number $\text{Pm} = \text{Rm}/\text{Re} \approx \nu/\eta$. We study two cases for the Prandtl number: a case when it is large and a case when it is small. In the first case, $\text{Pm} \sim 150 \gg 1$, which is achieved by choosing $k_{\text{max}} = 3000$ ($\text{Re} \sim 6800$). In the second case, $\text{Pm} \sim 6.7 \times 10^{-4} \ll 1$, which corresponds to our choice $k_{\text{max}} = 3 \times 10^7$ ($\text{Re} \sim 1.5 \times 10^9$). These two cases of large and small Prandtl numbers are considered in combination with two cases for the kinetic helicity: first, a case when $h = 1$ in Equation (8) and the velocity field is maximally helical and second, a case when $h = 0.1$ and the kinetic helicity is small. Thus, in total we consider four cases for our choice of the Prandtl number Pm and the kinetic helicity parameter h . The resulting growth rates λ_n of the bound (localized) eigenmodes and λ_0 of the fastest growing unbound (nonlocalized) eigenmode are shown on the logarithmic-scale plots in Figure 1. The growth rates are measured in the units of large-scale eddy turnover rate $\sim v_0/l_0$ ($v_0/l_0 \sim 1$ here). The logarithmic-scale plots of the absolute values of magnetic energy spectral eigenfunctions are given in Figure 2. The logarithmic-scale plots of the absolute values of electric current helicity spectral eigenfunctions are given in Figure 3.

In the case $\text{Pm} \sim 150$ and $h = 1$ there exist 10 growing bound eigenmodes of magnetic field, whose growth rates are shown on the plot (A) in Figure 1. Among these we select four bound modes $\lambda_1 \simeq 35.41$, $\lambda_2 \simeq 42.74$, $\lambda_7 \simeq 213.4$, and $\lambda_{10} \simeq 731.1$, and we plot their magnetic energy and current helicity spectral eigenfunctions by the dotted, dash-dotted, dashed, and smooth solid lines, respectively, on the left-upper plots in Figures 2 and 3. The spectral eigenfunctions of the fastest unbound eigenmode $\lambda_0 \simeq 33.23$ are shown by the red jagged spiky lines on these left-upper plots. In the case $\text{Pm} \sim 150$ and $h = 0.1$ there are just four bound magnetic field eigenmodes, which are shown on the plot (B) in Figure 1. These eigenmodes are $\lambda_1 \simeq 0.3336$, $\lambda_2 \simeq 26.03$, $\lambda_3 \simeq 190.1$, and $\lambda_4 \simeq 654.2$, and their energy and helicity spectral eigenfunctions are shown by the dotted, dash-dotted, dashed, and smooth solid lines on the right-upper plots in Figures 2 and 3. The fastest growing unbound eigenmode grows at a rate $\lambda_0 \simeq 0.3323$, and its spectral eigenfunctions are shown by the red jagged spiky lines. Next, in the case $\text{Pm} \sim 6.7 \times 10^{-4}$ and $h = 1$ there are eighteen bound magnetic eigenmodes in total, all are shown on the plot (C) in Figure 1. The spectral eigenfunctions of four selected bound eigenmodes $\lambda_1 \simeq 41.73$, $\lambda_2 \simeq 49.56$, $\lambda_{10} \simeq 695.9$, and $\lambda_{18} \simeq 17055$ are shown by the dotted, dash-dotted, dashed, and smooth solid lines on the left-lower plots in Figures 2 and 3. The spectra of the fastest growing unbound mode $\lambda_0 \simeq 39.57$ are again shown by the red jagged spiky lines. Finally, in the case $\text{Pm} \sim 6.7 \times 10^{-4}$ and $h = 0.1$ there are four bound eigenmodes, $\lambda_1 \simeq 0.39581$, $\lambda_2 \simeq 12.30$, $\lambda_3 \simeq 103.5$, and $\lambda_4 \simeq 669.8$, refer to the plot (D) in Figure 1. These four modes and the fastest growing unbound mode $\lambda_0 \simeq 0.39573$ have spectra that are shown on the right-lower plots in Figures 2 and 3 by the dotted, dash-dotted, dashed, smooth solid, and red jagged

spiky lines, respectively.

Based on the results presented in Figures 1–3, we make the following important observations.

First, when the kinetic helicity increases, the number of bound magnetic eigenmodes increases significantly. Their growth rates, λ_n , become strongly concentrated near the growth rate of the fastest unbound eigenmode, λ_0 . (This last result follows from a nearly uniform distribution of λ_n on the logarithmic-scale plots (A) and (C) in Figure 1.)

Second, on all plots in Figure 1 the growth rate of the first bound eigenmode, λ_1 , happens to be very close to λ_0 . We found same result for all other high Reynolds number cases that we investigated (not reported here), with different admissible values of the helicity parameter h . Thus, we propose that for dynamo driven by high Reynolds number Kolmogorov-type velocity field there always exists a shallow bound eigenmode λ_1 , such that $\lambda_1 - \lambda_0 \ll \lambda_0$. This shallow mode grows faster than any of the unbound modes because $\lambda_1 > \lambda_0$.

Third, the spectra of the shallow bound eigenmode λ_1 , shown by the dotted lines in Figures 2 and 3, and the spectra of the fastest growing unbound eigenmode λ_0 , shown by the red jagged spiky lines, are close near the magnetic energy containing large scales. (Small-scale structures of these modes are however different: the shallow eigenmode has a relatively larger small-scales component.) In practical applications, the shallow mode grows faster than the unbound modes and can dominate at large scales; however it cannot be described by the conventional α -model for large-scale dynamo, since this model does not capture the bound modes.

Fourth, consider the spectra of eigenmodes λ_0 and λ_1 (the dotted lines and the red jagged spiky solid lines in Figures 2 and 3). When the value of the kinetic helicity drops by a factor of 10 (from $h = 1$ to $h = 0.1$), the location of the peaks of these spectra shifts to larger scales by the same factor. Thus, the characteristic scales of eigenmodes λ_0 and λ_1 are both approximately equal to $\sim l_0/h$, so that both these modes peak at large scale when kinetic helicity is small.³ This result is consistent with general predictions of the α -model (Steenbeck, Krause & Radler 1966).

³ At large correlation scales $x \rightarrow \infty$, the eigenfunction of the fastest growing unbound eigenmode, $\lambda_0 = g^2(0)/[\kappa_L(0) + 2\eta] \sim h^2 v_0/l_0$, asymptotically becomes a mixture of cosine and sine standing waves with wavenumber $k_0 = \sqrt{\lambda_0/\sqrt{\kappa_L(0) + 2\eta}} \sim h/l_0$, while the bound eigenfunctions decline as $\propto \exp(-\mu_n x)$, where $\mu_n = \sqrt{\lambda_n - \lambda_0/\sqrt{\kappa_L(0) + 2\eta}}$ (Boldyrev, Cattaneo & Rosner 2005; Malyshkin & Boldyrev 2007).

4. Conclusion

We have presented the full numerical characterization of the kinematic Kazantsev-Kraichnan dynamo model in the case of the Kolmogorov scaling of the velocity field. Our main conclusion is that the structure and the characteristic correlation scales of the magnetic field amplified by helical kinematic dynamo action are determined by both bound (localized) and unbound (nonlocalized) growing eigenmodes. In particular, the large-scale component of the field is defined by the unbound eigenmodes and by the shallow bound eigenmodes. Because these shallow bound eigenmodes have growth rates higher than those of all unbound eigenmodes, at any given scale the former may rapidly become dominant over the latter. In practical applications, this means that the shallow bound modes, rather than the unbound modes, are likely to become essential in the large-scale magnetic field configurations in astrophysical systems. In this case the conventional α -dynamo model (Steenbeck, Krause & Radler 1966; Moffatt 1978; Kulsrud 2005) gives an inadequate description of the large-scale magnetic field even at the kinematic stage of dynamo action.

The α -model becomes inapplicable in this case because it uses a critical assumption that small-scale fluctuations of the velocity and magnetic fields are much weaker and concentrated at the scales much smaller than the scales of the growing large-scale field. Under this assumption the α -model is obtained by averaging the induction Equation (1) over these small-scale fluctuations to obtain a linear and homogeneous differential equation for the large-scale mean magnetic field.⁴ Thus, the α -model misses all growing bound magnetic eigenmodes, including the essential shallow bound eigenmodes that determine the eventual large-scale configuration of the magnetic field.

We thank Fausto Cattaneo for many useful and stimulating discussions. This work was supported by the NSF Center for Magnetic Self-Organization in Laboratory and Astrophysical Plasmas at the Universities of Chicago and Wisconsin-Madison. S.B. is supported by the U.S. Department of Energy under the grant no. DE-FG02-07ER54932.

REFERENCES

- Blackman, E. G., & Field, G. B. 2002, *ApJ*, **572**, 685
- Boldyrev, S., & Cattaneo, F. 2004, *Phys. Rev. Lett.*, **92**, 144501

⁴The α -model equation for the mean field $\overline{\mathbf{B}}$ is $\partial_t \overline{\mathbf{B}} = \alpha \nabla \times \overline{\mathbf{B}} + \beta \nabla^2 \overline{\mathbf{B}}$. This is a linear and homogeneous differential equation with constant coefficients $\alpha \sim \mathbf{v} \cdot (\nabla \times \mathbf{v}) \tau_0$ and $\beta \sim v_0 l_0$, where v_0 is a characteristic velocity, l_0 is a characteristic scale, and $\tau_0 \sim l_0/v_0$ is a characteristic decorrelation time of fluid fluctuations.

- Boldyrev, S., Cattaneo, F., & Rosner, R. 2005, *Phys. Rev. Lett.*, **95**, 255001
- Brandenburg, A., & Subramanian, K. 2005, *Phys. Rep.*, **417**, 1
- Frisch, U. 1995, *Turbulence* (Cambridge: Cambridge Univ. Press.)
- Haugen, N.E.L., Brandenburg, A., Dobler, W. 2004, *Phys.Rev. E*, **70**, 016308
- Kazantsev, A. P. 1968, *JETP*, **26**, 1031
- Kim, E., & Hughes, D. W. 1997, *Phys. Lett. A*, **236**, 211
- Kraichnan, R. H., *Phys. Fluids* 1968, **11**, 945
- Kulsrud, R. M. 2005, *Plasma Physics for Astrophysics* (Princeton, NJ: Princeton Univ. Press)
- Kulsrud, R. M., & Anderson, S. W. 1992, *ApJ*, **396**, 606
- Kulsrud, R. M., and Zweibel, E. G. 2008, *Rep. Prog. Phys.*, **71**, 046901
- Lynden-Bell, D. (ed.) 1994, *Cosmical Magnetism* (Dordrecht: Kluwer)
- Malyshkin, L., & Boldyrev, S. 2007, *ApJ*, **671**, L185
- Maron, J. & Cowley, S. 2001, arXiv:astro-ph/0111008
- Moffatt, H. K. 1978, *Magnetic Field Generation in Electrically Conducting Fluids* (Cambridge University Press)
- Monin, A. S., & Yaglom, A. M. 1971, *Statistical Fluid Mechanics* (Cambridge, MA: MIT Press)
- Parker, E. N. 1979, *Cosmical Magnetic Fields* (Oxford: Clarendon)
- Schekochihin, A. A., & Cowley, S. C. 2006, *Astron. Nachr.*, **327**, 599
- Steenbeck, M., Krause, F., & Radler, K. H. 1966, *Z. Naturforsch.*, **21a**, 369
- Vainshtein, S. I., & Kichatinov, L. L. 1986, *J. Fluid Mech.*, **168**, 73
- Vainshtein, S. I., & Zeldovich, Ya. B. 1972, *Sov. Phys.–Usp.*, **15**, 159
- Zweibel, E. G., & Heiles, C. 1997, *Nature*, **385**, 131

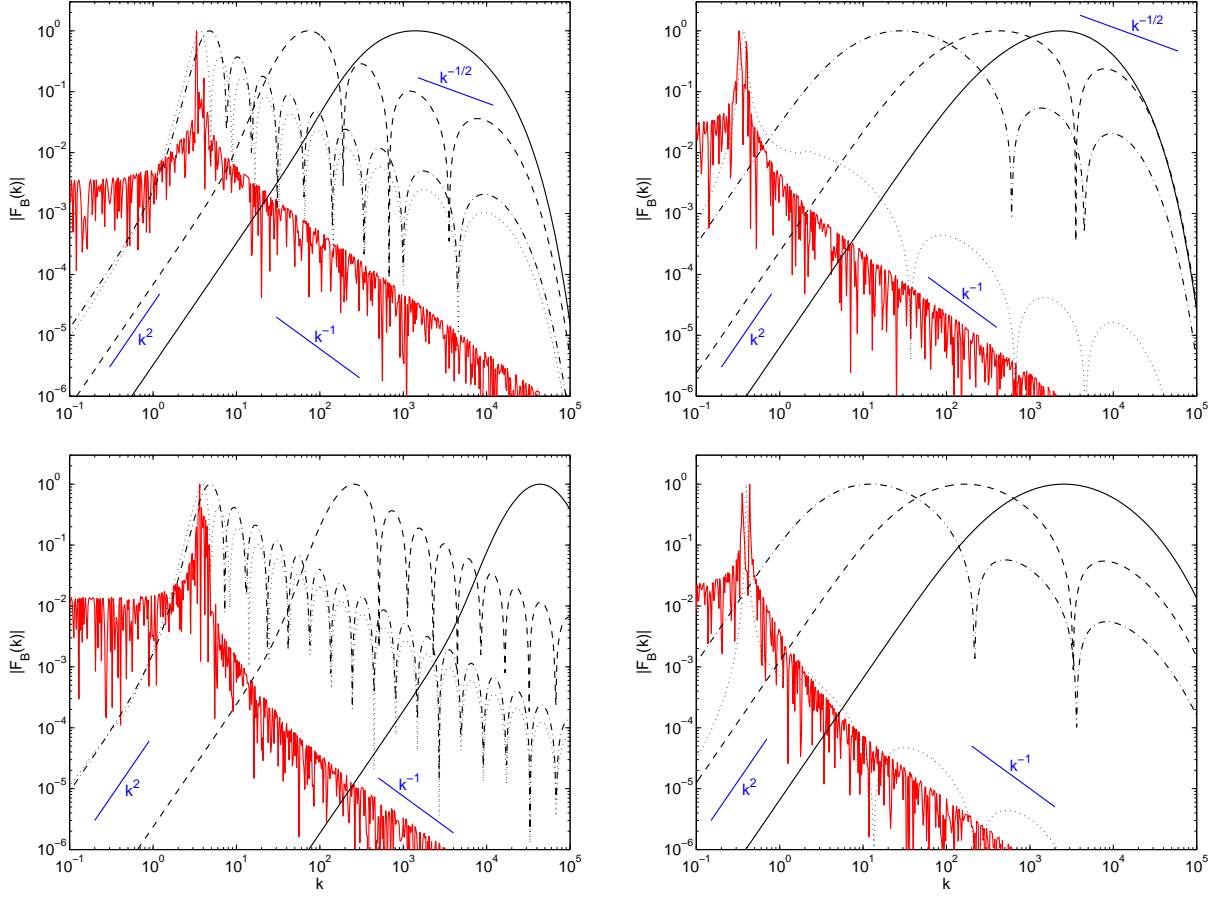


Fig. 2.— Absolute values of magnetic energy spectral eigenfunctions for four selected bound eigenmodes (shown by the dotted, dash-dotted, dashed, and smooth solid lines), and for the fastest growing unbound eigenmode (shown by the red jagged spiky solid lines). The left-upper, right-upper, left-lower, and right-lower plots are for the cases $\text{Pm} \sim 150$ & $h = 1$, $\text{Pm} \sim 150$ & $h = 0.1$, $\text{Pm} \sim 6.7 \times 10^{-4}$ & $h = 1$, and $\text{Pm} \sim 6.7 \times 10^{-4}$ & $h = 0.1$, respectively.

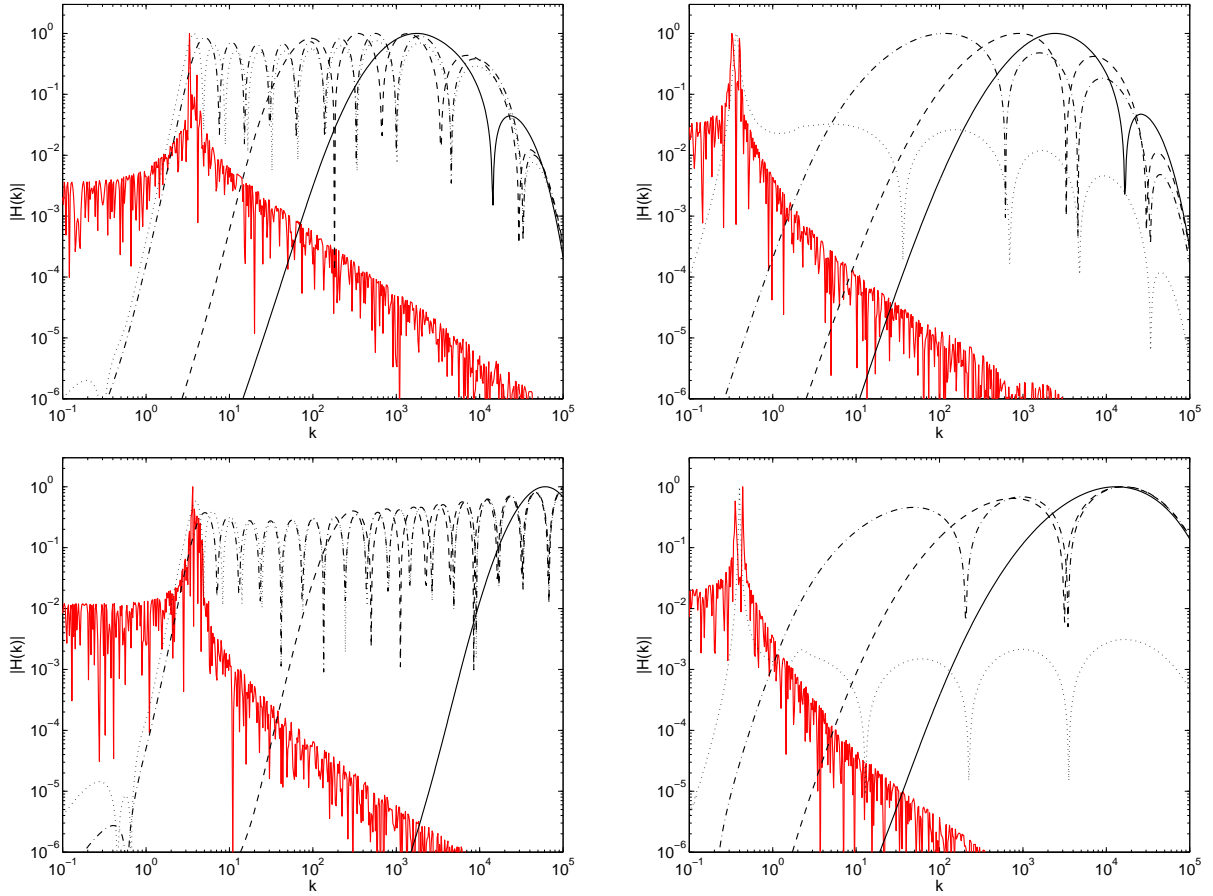


Fig. 3.— Same as Figure 2 except the absolute values of electric current helicity spectral eigenfunctions are plotted here.